Magnesium substitution in calcium and strontium fluoro-phospho-aluminosilicate glasses by multinuclear ^{19}F, ^{31}P, ^{27}Al, and ^{29}Si MAS-NMR spectroscopy

Hiroko Kusumoto[1], Robert G. Hill[3], Natalia Karpukhina[3], Robert V. Law[*2]

[1] *Department of Materials, Imperial College London, South Kensington Campus, London, SW7 2AZ, UK*

[2.] *Department of Chemistry, Imperial College London, South Kensington Campus, London, SW7 2AZ UK*

[3] *Dental Physical Sciences, Institute of Dentistry, Barts and The London School of Medicine and Dentistry, Queen Mary University of London, Mile End Road, London, E1 4NS, UK*

* Corresponding author:

Name: Robert V. Law

Address: Department of Chemistry, Imperial College London, South Kensington Campus, London, SW7 2AZ UK

Phone: +44-20-7594-5860

E-mail: r.law@imperial.ac.uk

Abstract

Two series of glasses were produced by systematically substituting magnesium for calcium and strontium in the glass compositions, $4.5SiO_2$. $3Al_2O_3$. $1.5P_2O_5$. $(3-x)CaO/SrO$. $xMgO$. $(2-y)CaF_2/SrF_2$. $yMgF_2$, and these glasses were characterised by ^{19}F, ^{31}P, ^{27}Al, and ^{29}Si MAS-NMR spectroscopy. The substitution of magnesium for calcium and strontium resulted in the gradual formation of F-Mg(n) species over the F-Ca(n) and F-Sr(n) with additional loss of Al-F species. The ^{31}P and ^{27}Al MAS-NMR spectra showed the presence of $Al-O-PO_3^{3-}$ species charge balanced by a mixture of Ca^{2+} and Mg^{2+} or Sr^{2+} and Mg^{2+}. In addition to that, the ^{31}P MAS-NMR spectrum of the fully magnesium substituted glass showed the presence of amorphous magnesium pyrophosphate, $Mg_2P_2O_7$. Al(IV) was the major Al species with small amount of Al(V) and Al(VI), but the amount of Al(V) increased with increase in magnesium substitution. Moreover, the fully magnesium substituted fluoro-phospho-aluminosilicate glass resulted in the more polymerised silicate network with increased number of the bridging oxygen on SiO_4 tetrahedra.

Keywords: MAS-NMR, aluminosilicate glass, magnesium, calcium, strontium

Introduction

Glass ionomer (polyalkenoate) cements, GICs or GPC, have been used in dentistry since 1970's. They are formed by the acid-base reaction between a fluoro-aluminosilicate glass, also called ionomer or ion leachable glass, and poly(carboxylic acid), usually poly(acrylic acid) [1]. During the cement formation, ions such as Ca^{2+} or Sr^{2+} and Al^{3+} are released to form ionic crosslinks with carboxylate groups in the polymeric acrylic acid [1]. The structure of these fluoro-aluminosilicate glasses, used for GICs, have been already studied using magic angle spinning-nuclear magnetic resonance (MAS-NMR) spectroscopy [2-6]. However, no previously the studied formulations contain magnesium.

As the ionic size of Mg^{2+} is smaller than Ca^{2+} and Sr^{2+}, it possess a higher charge density, and therefore the carboxylate groups will be brought closer together during the cement formation when crosslinked using Mg^{2+} in comparison to Ca^{2+} and Sr^{2+}, altering the mechanical properties of the cements. The calcium containing glass compositions studied here are based on the composition known as LG26 [$4.5SiO_2$. $3Al_2O_3$. $1.5P_2O_5$. $3CaO$. $2CaF_2$], and this glass is commercially used in the GICs for dental and medical applications. Fully substituted strontium version of the LG26 glass, known as LG26Sr [$4.5SiO_2$. $3Al_2O_3$. $1.5P_2O_5$. $3SrO$. $2SrF_2$], was the starting formulation for the Sr-Mg series of glasses, which was parallel to the Ca-Mg series and is also presented here. Strontium instead calcium is often used in formulations of the ionomer or ion leachable glasses mostly because it make the cements made of these formulations radiopaque.

Calcium in LG26 and strontium in LG26Sr were substituted by magnesium on a mole basis, and the structure of the magnesium containing glasses was investigated by solid state MAS-NMR spectroscopy. We believe that the glass structure determines its property, and therefore, by applying the MAS-NMR technique to study the structure of the magnesium containing glasses, the properties of the GPCs can be improved.

This study also looked at the role of Mg^{2+} in these ionomer glasses. Magnesium is known to be an intermediate between the network forming and network modifying actions in silicate glasses and its role in glass structure has been often controversial and varies depending on the glass compositions. For example, Fayon *et al.* [7] studied various magnesium phosphate glasses, $(MgO)_x(P_2O_5)_{1-x}$ using ^{31}P MAS-NMR and showed that Mg^{2+} is a network modifying cation near the metaphosphate compositions, ranging from x=0.44 to 0.55. Gervais *et al*. [8] used infrared spectroscopy and found that Mg^{2+} in silicate glasses forms a network, like SiO_2, in the $MgO-Al_2O_3-SiO_2$ system.

Experimental

Glass Synthesis

The glass compositions are tabulated in Table 1. The glasses were designed so that the total cation (Mg+Ca:F) ratio to the network forming Al:Si:P was constant. The analytical grade reagents were weighed and mixed in a plastic container. The mixed powder was melted in a platinum/rhodium crucible in the furnace at required temperatures (1420-1475°C) for 1.5 hrs. The melt was then poured rapidly into water to prevent crystallisation. The resulting frit was dried overnight in an oven at 100 ˚C, and 100 g of the dried frit was ground using Gyro Mill (Glen Creston Gyro Mill,

Middlesex, England) to obtain glass powder. The XRD results revealed that all the glasses from both series were amorphous.

Table 1. Glass compositions in mol %.

Series	Code	SiO_2	Al_2O_3	P_2O_5	CaO	CaF_2	MgO	MgF_2	Mg:F	Ca:F
Ca-Mg	LG26	32.1	21.4	10.7	21.4	14.3	---	---	---	5.0
	ICHK02	32.1	21.4	10.7	16.1	14.3	5.4	---	0.7	4.3
	ICHK03	32.1	21.4	10.7	10.7	14.3	10.7	---	1.5	3.5
	ICHK04	32.1	21.4	10.7	21.4	---	---	14.3	2.0	3.0
	ICHK05	32.1	21.4	10.7	---	14.3	21.4	---	3.0	2.0
	ICHK06	32.1	21.4	10.7	10.7	---	10.7	14.3	3.5	1.5

Series	Code	SiO_2	Al_2O_3	P_2O_5	SrO	SrF_2	MgO	MgF_2	Mg:F	Sr:F
Sr-Mg	LG26Sr	32.1	21.4	10.7	21.4	14.3	---	---	---	5.0
	ICHK08	32.1	21.4	10.7	16.1	14.3	5.4	---	0.7	4.3
	ICHK09	32.1	21.4	10.7	10.7	14.3	10.7	---	1.5	3.5
	ICHK10	32.1	21.4	10.7	21.4	---	---	14.3	2.0	3.0
	ICHK11	32.1	21.4	10.7	---	14.3	21.4	---	3.0	2.0
	ICHK12	32.1	21.4	10.7	10.7	---	10.7	14.3	3.5	1.5
	LG26Mg	32.1	21.4	10.7	---	---	21.4	14.3	5.0	---

Glass Characterisation

MAS-NMR was performed on the ^{19}F, ^{31}P, ^{27}Al, and ^{29}Si nuclei using the 200 MHz (4.7 T) solid state NMR spectrometer for ^{19}F, ^{31}P, and ^{29}Si, and the 600 MHz (14.1 T) for ^{27}Al. The resonance frequencies were 188.3, 80.9, 39.8 and 156.3 MHz and the spinning rates were 4-15 kHz for ^{19}F, ^{31}P, ^{29}Si, and ^{27}Al nuclei respectively. The recycle times were 10.0, 2.0, 1.0, and 2.0s for ^{19}F, ^{31}P, ^{27}Al and ^{29}Si respectively. A 4 mm zirconia rotor was used. Single pulse corresponding to 60-80 kHz of radiofrequency field was used across the experiments for all nuclei. The short pulse 0.3 μs was applied in ^{27}Al NMR experiments corresponding to $\pi/12$ of the magnetization tip angle. The ^{19}F NMR spectra were obtained after subtraction the background spectrum acquired individually on a sample free rotor prior to each sample run. 1 M solution of NaF producing a signal at -120 ppm was used to reference the ^{19}F NMR chemical shift scale. 85 % H_3PO_4 and 1 M $Al(NO_3)_3$ solutions were used to reference ^{31}P and ^{27}Al NMR chemical shift respectively. The ^{29}Si resonance signal from (tetrakis)trimethylsilylmethane ($C(Si(CH_3)_3)_4$) at -1.5 ppm was used for referencing the ^{29}Si NMR chemical shift.

Results and Discussion

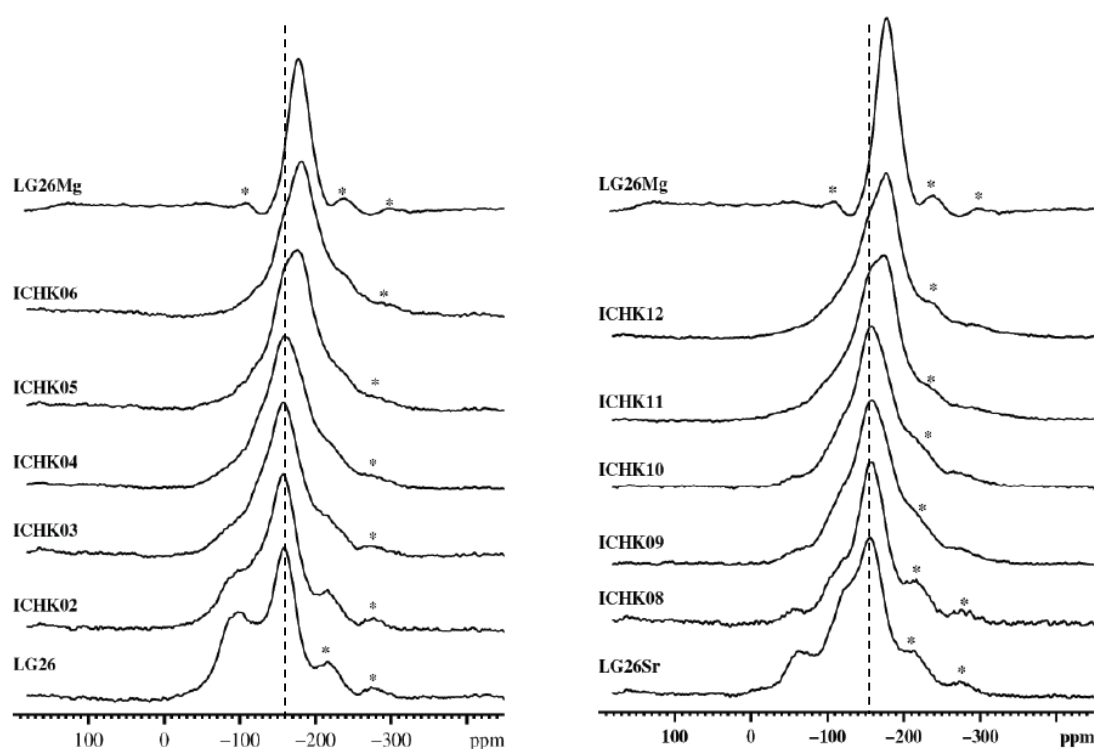### ^{19}F MAS-NMR spectroscopy

Figure 1. ^{19}F MAS-NMR spectra for the Ca-Mg (left) and Sr-Mg (right) series with the spinning side bands marked by asterisks. The spinning speed 12kHz was used.

Glass LG26 exhibited two main peaks in the ^{19}F MAS-NMR spectra with the positions at -98 and -159 ppm (left, Figure 1), which have been assigned to F-Ca(n) and Al-F-Ca(n) species. Similarly, the composition LG26Sr showed two main peaks at -62 and -156 ppm (right, Figure 1), and these peaks have been assigned to F-Sr(n) and Al-F-Sr(n) species, respectively [2]. The F-Ca(n) and F-Sr(n) species contain F in close proximity to and charge balanced by Ca^{2+} and Sr^{2+} and these fluoride species are not part of the silicate glass network. The fluoride in the Al-F-Ca(n) and Al-F-Sr(n) species is attached to Al in the glass network and is in close proximity to Ca^{2+} and Sr^{2+} as well [2, 9]. In addition to these main peaks both LG26Sr and ICHK08 show an additional signal at -130 ppm, that is particularly clear in the LG26Sr composition spectrum. This

signal was assigned to the fluoride from the F-Al-O-PO$_3^{3-}$ species as was proposed previously [10].

The chemical shift for F-Sr(n) species in the fully strontium substituted glass LG26Sr is less negative than for F-Ca(n) species. According to Bureau et $al.$ [11], the increase in the chemical shift from F-Ca(n) to F-Sr(n) species is due to an increase in the distance between the divalent cation and F$^-$ due to a slightly larger cationic radius of Sr^{2+} compared to the Ca^{2+}.

The both F-Ca(n) and F-Sr(n) signals start to reduce in intensity on magnesium substitution. Glass compositions ICHK02 in the Ca-Mg series and ICHK08 in the Sr-Mg series contain the same amount of magnesium. However, the F-Sr(n) intensity in ICHK08 is much smaller than the F-Ca(n) intensity in the ICHK02. This suggests that Mg^{2+} takes fluoride away from Sr^{2+} in the Sr-Mg series more efficiently than from the Ca^{2+} in the Ca-Mg series, which is due to the lower field of strontium cation compared to the field strength of the Ca^{2+}.

With further magnesium substitution, in the compositions ICHK03, ICHK04 and ICHK09, ICHK10, the Al-F-Ca(n) and Al-F-Sr(n) species with the signal at ca. -160 ppm become dominant in the ^{19}F MAS-NMR spectra. Eventually, the signal at -176 ppm in the Ca-Mg series and at -179 ppm in the Sr-Mg series that was seen first appearing as a shoulder on increase in magnesium content in both series (ICHK05, ICHK11) becomes the principal signal in the LG26Mg composition. This signal is assigned to F-Mg(n) species, with n $\sim$ 3, indicating that there are possibly three Mg surrounding F [11, 12]. The fact that F-Mg(n) species is solely formed in both series indicates that F attaches preferentially to Mg rather than Al, and a similar observation was reported by Labouriau [13]. F-Mg(n) species are probably favoured by the higher charge to size ratio of Mg^{2+} relative to Ca^{2+}. Stebbins and Zeng [9] has suggested that

fluorine preferentially attaches to cations of highest charge to size ratio. Reconstruction of the spectra with amorphous ^{19}F signal was shown to be highly ambiguous even in the aluminium free silicate glasses [14], therefore was not attempted here.
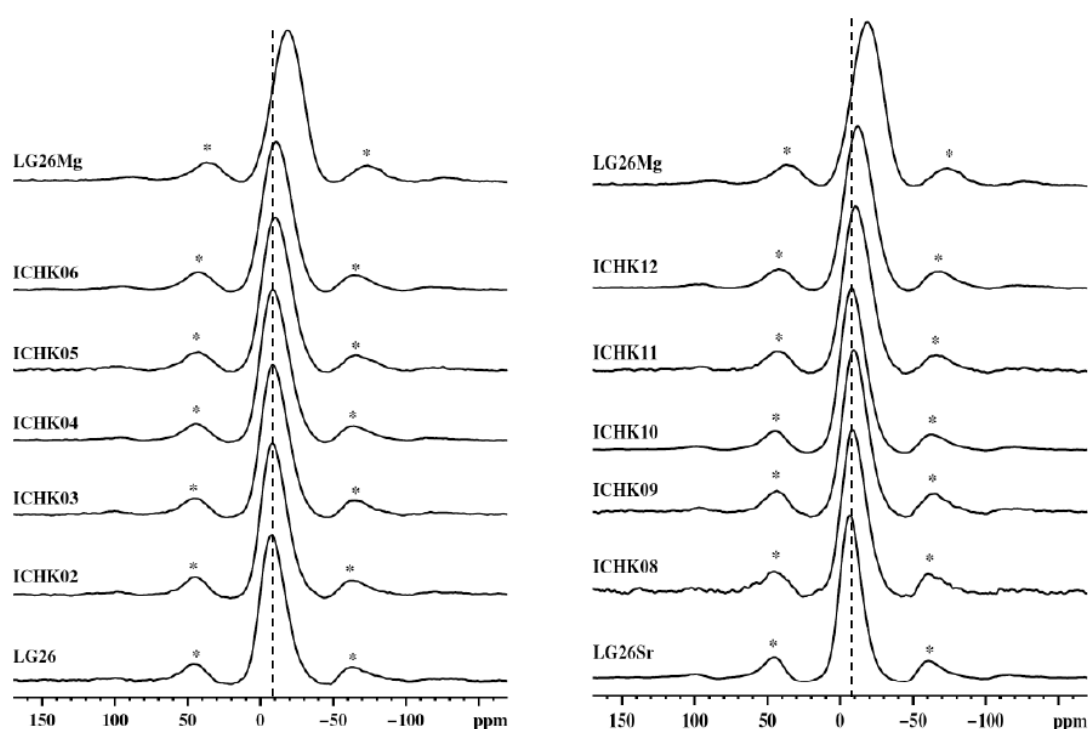
^{31}P MAS-NMR spectroscopy

Figure 2. ^{31}P MAS-NMR spectra for the Ca-Mg (left) and Sr-Mg (right) series with the spinning side bands marked by asterisks. The spinning speed of 4.5kHz was used.

Glass LG26 exhibited a single peak at -8 ppm (Figure 2, left) and glass LG26Sr showed a peak at -7 ppm (Figure 2, right); both of which have been assigned to Q^1 pyrophosphate Al-O-PO_3^{3-} species, with the non-bridging oxygens on phosphorus charge balanced by Ca^{2+} or Sr^{2+} [2, 3, 6, 15]. Slightly less negative chemical shift of the ^{31}P signal in the Sr-Mg series than in the LG26 is thought to be due to a small difference

in the field strength of Sr^{2+} and Ca^{2+} and have been also observed by Zainuddin *et al.* [16].

As calcium and strontium are substituted by magnesium, the ^{31}P chemical shift becomes more negative, moving away from 0 ppm, as can be also seen from the plot in Figure 3. This shows that before full magnesium substitution occurs, the decrease in the peak position of the broad peak shifts in a consistent manner to show the formation of pyrophosphate in both series. However, the peak position seen in the LG26Mg glass, -19 ppm, does not fit the continuing trend. We propose that in the absence of other modifier cations, magnesium pyrophosphate is formed in this composition. The two signals at -12 and -19 ppm [17] are known for the amorphous magnesium pyrophosphate α-$Mg_2P_2O_7$ shown schematically in Figure 4. The ^{31}P signal for the LG26Mg is the broadest in the both series and most likely is resulted from overlap of several signals including phosphate species in magnesium pyrophosphate and Al-O-PO_3^{3-}. Due to featureless lineshape of the broad signal of the ^{31}P MAS-NMR spectra their further deconvolution was not attempted.
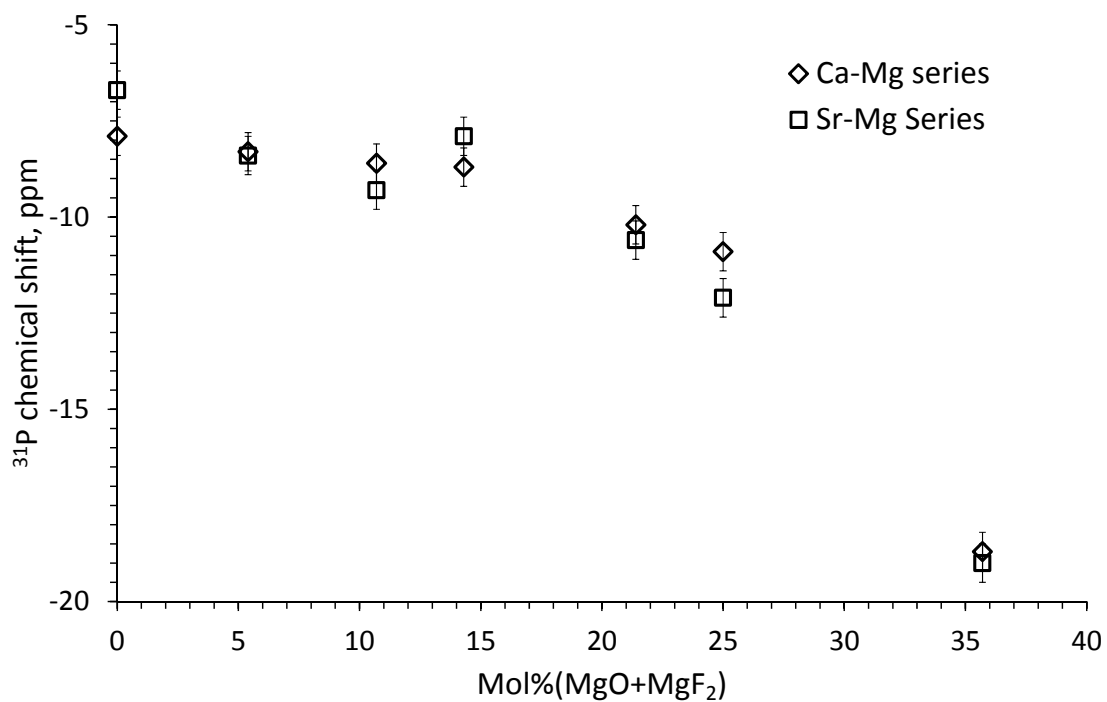
Figure 3. ^{31}P peak position values for the Ca-Mg and Sr-Mg series plotted against total Mg content in mol%
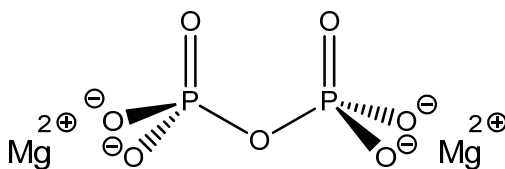

Figure 4. Schematic of magnesium pyrophosphate, Mg$_2$P$_2$O$_7$
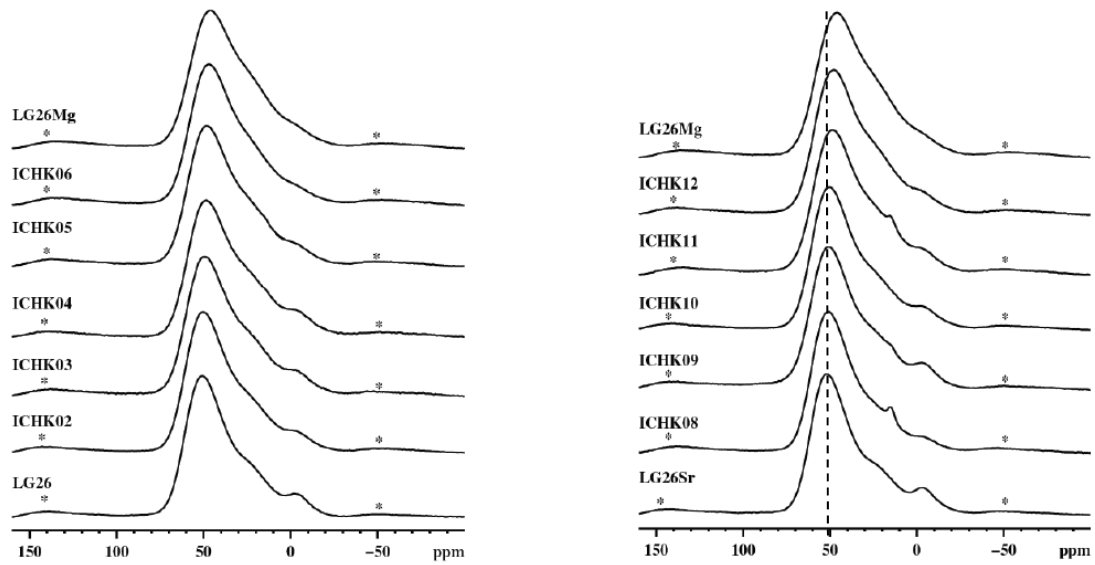
^{27}Al MAS-NMR spectroscopy

Figure 5. ^{27}Al MAS-NMR spectra for the Ca-Mg (left) and Sr-Mg (right) series with the spinning side bands marked by asterisks. The spinning speed of 15 kHz was used.

The ^{27}Al MAS-NMR spectra for both series showed a typical broad peak at 51-52 ppm (Figure 5) that shifted gradually towards 0ppm on magnesium substitution. The peak position for the LG26Mg glass was 45.8 ppm. This peak has been assigned to Al in tetrahedral coordination, Al(IV) [3, 6, 15]. All the glasses showed a shoulder on the Al(IV) peak at ca. 30 ppm and a small peak at ca. -5 ppm (Figure 5). These have been assigned to Al in pentahedral coordination, Al(V), and Al in octahedral coordination, Al(VI), respectively [18]. These ^{27}Al MAS-NMR spectra were deconvoluted using *dmfit* software[19] using the Cz model and the results are given in Table 2.

The data show that two series are very similar indicating that strontium instead of calcium in these glasses does not give any additional effect. The shift of the Al(IV) signal towards 0 ppm is explained by the formation of the Al-O-P linkages which has been previously observed in these systems [15, 20, 21]. The structure moieties with Al-O-P linkages are schematically illustrated in Figure 6.

Table 2. Fractions of three aluminium coordination species obtained from the deconvolution the spectra in Figure 5. The numbers before slash is for the Ca-Mg series and after the slash for the Sr-Mg series

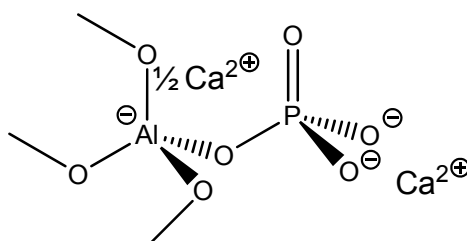| Glass code	Mg content /mol %	Mg substitution /%	Al(IV)/%	Al(V)/%	Al(VI)/%
LG26/LG26Sr	0.0	0	72/72	22/21	6/7
ICHK02/ICHK08	5.4	15	71/75	24/21	5/4
ICHK03/ICHK09	10.7	30	68/70	26/24	6/6
ICHK04/ICHK10	14.3	40	67/71	27/24	6/5
ICHK05/ICHK11	21.4	60	68/68	27/27	5/5
ICHK06/ICHK12	25.0	70	68/68	27/27	5/5
LG26Mg	35.7	100	65/65	29/29	6/6

Figure 6. A cartoon of the structural moieties with Al-O-P linkages in the calcium phospho-aluiminosilicate glasses

There is an increase in Al(V) species when magnesium fully substitutes calcium in LG26Mg. The increase in Al(V) species with magnesium containing aluminosilicate glass has also been found in various studies and has been suggested due to the higher cation field strength of Mg^{2+} than Ca^{2+} [20, 22]. This increase in the Al(V) species could have resulted in the shift of the Al(IV) peak for LG26Mg to a less positive value by

superposition of Al(IV) peak into the Al(V) peak. The role of Al(V) and Al(VI), whether they act as network forming or modifying, has been controversial [23].

In addition, the compositions ICHK08 and ICHK11 from the Sr-Mg series exhibited a small signal at 15 ppm. Similar signal has been also observed previously [16]. The low intensity and random appearance in the compositions series suggests that this is an impurity signal, though the origin of it remains unclear. It is possible that this signal is due to a minute crystalline impurity, maybe α-Al_2O_3, that was much below the detection limit of the XRD.

^{29}Si MAS-NMR spectroscopy

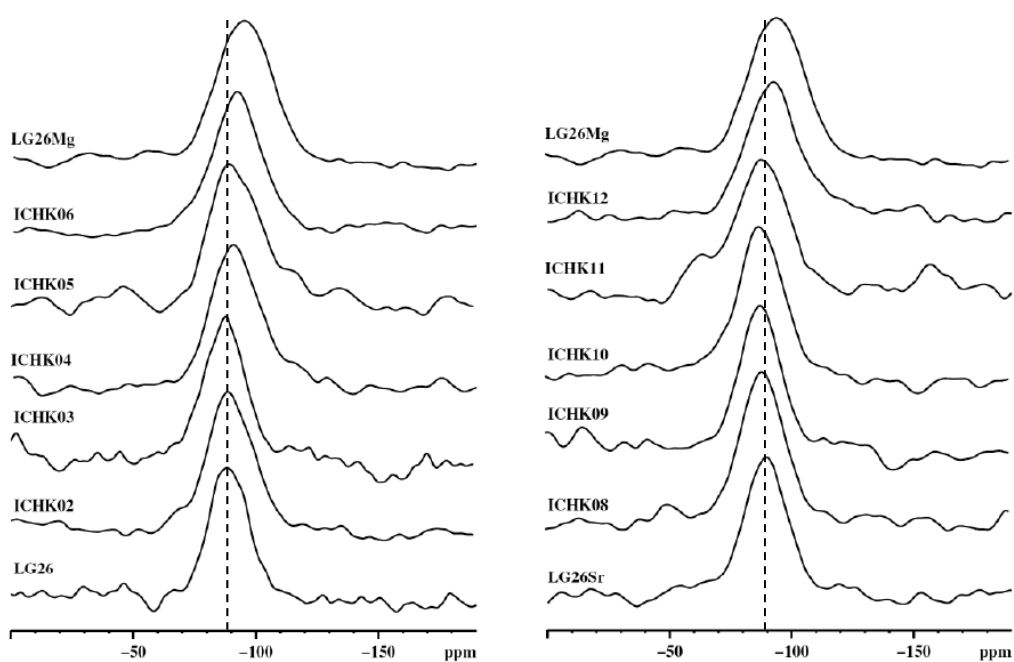**Figure 7. ^{29}Si MAS-NMR spectra for the Ca-Mg (left) and Sr-Mg (right) series. The spinning speed of 4.5 kHz was used.**

The ^{29}Si MAS-NMR spectra of the glasses showed a broad peak, initially at -89 and -90 ppm in the LG26 and LG26Sr correspondingly (Figure 7) which indicates that this glass contains a mixture of Q structures, namely Q^4(4Al) and Q^3(3Al) [2, 3, 15]. The peak shifts slightly towards more negative chemical shift values, moving away from 0 ppm with magnesium substitution for calcium and for strontium (Figure 7), and a similar trend was seen in previous studies [21, 24]. There was some difference between the Ca-Mg and Sr-Mg series, indicating that a high magnesium contents for each series (ICHK05, 06 and LG26Mg), (ICHK10, 11, 12, LG26Mg) in these silicate glasses appears to cause polymerisation of the network. It is also worth to pointing out, that the substitution of calcium and strontium by magnesium seems to broaden the peaks (Figure 7), and similar trends have been observed in several studies [21, 24].

A structure of aluminosilicate glasses can be expressed as $Si(OSi)_{m-n}(OAl^-)_n(O^-)_{4-m}$, ($Q^m(n\text{Al})$, $4 \geq m \geq n \geq 0$), where m is the number of bridging oxygen per SiO_4 unit and n the number of Al connected by oxygen with SiO_4 unit. It has been stated that the chemical shift increases as m is decreased or n is increased [25]. The ^{19}F MAS-NMR spectra (Figure 1) have shown that Mg^{2+} ions are used in forming F-Mg(n) species and are not available for charge balancing the non-bridging oxygens on the silicon. Moreover, ^{31}P MAS-NMR (Figure 2) has shown the possible formation of Mg pyrophosphate species (Figure 3) which will interact the available Mg^{2+} ions. Therefore, it is not possible to form any non-bridging oxygens on Si, and hence the number of bridging oxygens on Si increases forming more of Q^4 species. The ^{27}Al MAS-NMR spectra of the both series (Figure 5) showed that there is an increased amount of Al(V) and a decreased amount of Al(IV) species. Therefore, the decrease in the ^{29}Si chemical

shift for LG26Mg may also have resulted from the polymerisation of the silica network because more cations are associated with the F species. The broadening of the ^{29}Si peak may be due to the presence of Q^4 species with different number of Al next to SiO4.

Conclusion

The structures of magnesium containing fluoro-aluminosilicate glasses were analysed by ^{19}F, ^{31}P, ^{27}Al, and ^{29}Si MAS-NMR spectroscopy. ^{19}F MAS-NMR showed that fluorine preferentially attaches to magnesium forming F-Mg(n) species. ^{31}P MAS-NMR showed Q^1 pyrophosphate Al-O-PO$_3^{3-}$ species for the mixed Ca-Mg and Sr-Mg glasses, and an additional formation of Mg pyrophosphate, Mg$_2$P$_2$O$_7$ for the fully magnesium substituted glass. There was a reduction in the chemical shift for Al(VI) species in ^{27}Al MAS-NMR with magnesium substitution, but this may have resulted from the increase in Al(V) species. ^{29}Si MAS-NMR showed that the silicate network became more polymerised with magnesium substitution. Based on the results, we speculate, that compared to the modifier cations calcium and strontium in these glasses, the substituting Mg cation becomes more strongly associated with F and P in the fluoro-aluminosilicate glasses.

Acknowledgement

References

[1] A.D. Wilson, J.W. McLean, Glass-Ionomer Cement, Quinessense Publishing Co., Berlin, Germany, 1988.

[2] R.G. Hill, A. Stamboulis, R.V. Law, Characterisation of fluorine containing glasses by F-19, Al-27, Si-29 and P-31 MAS-NMR spectroscopy, J. Dent., 34 (2006) 525-532.

[3] S. Matsuya, A. Stamboulis, R.G. Hill, R.V. Law, Structural characterization of ionomer glasses by multinuclear solid state MAS-NMR spectroscopy, J. Non-Cryst. Solids, 353 (2007) 237-243.

[4] A. Stamboulis, R.G. Hill, R.V. Law, Characterization of the structure of calcium alumino-silicate and calcium fluoro-alumino-silicate glasses by magic angle spinning nuclear magnetic resonance (MAS-NMR), J. Non-Cryst. Solids, 333 (2004) 101-107.

[5] A. Stamboulis, R.V. Law, R.G. Hill, Characterisation of commercial ionomer glasses using magic angle nuclear magnetic resonance (MAS-NMR), Biomaterials, 25 (2004) 3907-3913.

[6] A. Stamboulis, R.G. Hill, R.V. Law, Structural characterization of fluorine containing glasses by F-19 Al-27 Si-29 and P-31 MAS-NMR spectroscopy, J. Non-Cryst. Solids, 351 (2005) 3289-3295.

[7] F. Fayon, D. Massiot, K. Suzuya, D.L. Price, P-31 NMR study of magnesium phosphate glasses, J. Non-Cryst. Solids, 283 (2001) 88-94.

[8] F. Gervais, A. Blin, D. Massiot, J.P. Coutures, M.H. Chopinet, F. Naudin, Infrared reflectivity spectroscopy of silicate-glasses, J. Non-Cryst. Solids, 89 (1987) 384-401.

[9] Q. Zeng, J.F. Stebbins, Fluoride sites in aluminosilicate glasses: High-resolution F-19 NMR results, Am. Miner., 85 (2000) 863-867.

[10] H. Kusumoto, Characterisation of Mg, Sr, and Zn containing fluoro-aluminosilicate glasses and their glass polyalkenoate cements, in: Materials, Imperial College London, 2009, pp. 207.

[11] B. Bureau, G. Silly, J.Y. Buzare, J. Emery, Superposition model for F-19 isotropic chemical shift in ionic fluorides: from basic metal fluorides to transition metal fluoride glasses, Chem. Phys., 249 (1999) 89-104.

[12] R.G. Hill, A. Stamboulis, R.V. Law, J. Hawes, J. Henry, MAS-NMR study of the crystallisation process of barium fluorphlogopite glass ceramics, Phys. Chem. Glasses, 45 (2004) 121-126.

[13] A. Labouriau, Y.W. Kim, S. Chipera, D.L. Bish, W.L. Earl, A F-19 nuclear magnetic resonance study of natural clays, Clay Clay Min., 43 (1995) 697-704.

[14] A. Pedone, T. Charpentier, M.C. Menziani, The structure of fluoride-containing bioactive glasses: new insights from first-principles calculations and solid state NMR spectroscopy, J. Mater. Chem., 22 (2012) 12599-12608.

[15] R.G. Hill, A. Stamboulis, R.V. Law, A. Clifford, M.R. Towler, C. Crowley, The influence of strontium substitution in fluorapatite glasses and glass-ceramics, J. Non-Cryst. Solids, 336 (2004) 223-229.

[16] N. Zainuddin, N. Karpukhina, R.G. Hill, R.V. Law, A long-term study on the setting reaction of glass ionomer cements by Al-27 MAS-NMR spectroscopy, Dent. Mater., 25 (2009) 290-295.

[17] M. Sadiq, M. Bensitel, C. Lamonier, J. Leglise, Influence of the nature of precipitating basic agent on the synthesis of catalytic magnesium phosphate materials, Solid State Sci., 10 (2008) 434-437.

[18] S.C. Kohn, R. Dupree, M.G. Mortuza, C.M.B. Henderson, Nmr evidence for 5-coordinated and 6-coordinated aluminum fluoride complexes in f-bearing aluminosilicate glasses, Am. Miner., 76 (1991) 309-312.

[19] D. Massiot, F. Fayon, M. Capron, I. King, S. Le Calve, B. Alonso, J.O. Durand, B. Bujoli, Z.H. Gan, G. Hoatson, Modelling one- and two-dimensional solid-state NMR spectra, Magn. Reson. Chem., 40 (2002) 70-76.

[20] K.E. Kelsey, J.R. Allwardt, J.F. Stebbins, Ca-Mg mixing in aluminosilicate glasses: An investigation using O-17 MAS and 3QMAS and Al-27 MAS NMR, J. Non-Cryst. Solids, 354 (2008) 4644-4653.

[21] G. Libourel, C.A. Geiger, L. Merwin, A. Sebald, Si-29 and al-27 mas-nmr spectroscopy of glasses in the system casio3-mgsio3-al2o3, Chemical Geology, 96 (1992) 387-397.

[22] S.K. Lee, G.D. Cody, B.O. Mysen, Structure and the extent of disorder in quaternary (Ca-Mg and Ca-Na) aluminosilicate glasses and melts, Am. Miner., 90 (2005) 1393-1401.

[23] D.R. Neuville, L. Cormier, D. Massiot, Al coordination and speciation in calcium aluminosilicate glasses: Effects of composition determined by Al-27 MQ-MAS NMR and Raman spectroscopy, Chemical Geology, 229 (2006) 173-185.

[24] C.I. Merzbacher, B.L. Sherriff, J.S. Hartman, W.B. White, A high-resolution si-29 and al-27 nmr-study of alkaline-earth aluminosilicate glasses, J. Non-Cryst. Solids, 124 (1990) 194-206.

[25] G. Engelhardt, M. Nofz, K. Forkel, F.G. Wihsmann, M. Magi, A. Samoson, E. Lippmaa, Structural studies of calcium aluminosilicate glasses by high-resolution solid-state si-29 and al-27 magic angle spinning nuclear magnetic-resonance, Phys. Chem. Glasses, 26 (1985) 157-165.

Figure 1. ^{19}F MAS-NMR spectra for the Ca-Mg (left) and Sr-Mg (right) series with the spinning side bands marked by asterisks. The spinning speed 12kHz was used.

Figure 2. ^{31}P MAS-NMR spectra for the Ca-Mg (left) and Sr-Mg (right) series with the spinning side bands marked by asterisks. The spinning speed of 4.5kHz was used.

Figure 3. ^{31}P peak position values for the Ca-Mg and Sr-Mg series plotted against total Mg content in mol %

Figure 4. Schematic of magnesium pyrophosphate, $Mg_2P_2O_7$

Figure 5. ^{27}Al MAS-NMR spectra for the Ca-Mg (left) and Sr-Mg (right) series with the spinning side bands marked by asterisks. The spinning speed of 15 kHz was used.

Figure 6. A cartoon of the structural moieties with Al-O-P linkages in the calcium phospho-aluiminosilicate glasses

Figure 7. ^{29}Si MAS-NMR spectra for the Ca-Mg (left) and Sr-Mg (right) series. The spinning speed of 4.5 kHz was used.

Table 2. Glass compositions in mol %.

Table 2. Fractions (%) of three aluminium coordination species obtained from the deconvolution the spectra in Figure 5. The numbers before slash is for the Ca-Mg series and after the slash for the Sr-Mg series

Highlights

- In fluoro-phospho-aluminosilicate glasses, the ^{19}F MAS-NMR revealed that the substitution of magnesium for calcium or strontium results in gradual formation of F-Mg(n) species over the F-Ca(n) or F-Sr(n) with additional loss of Al-F species.

- On magnesium substitution for calcium in fluoro-phospho-aluminosilicate glasses, the ^{31}P MAS-NMR spectra showed the presence of Al-O-PO$_3^{3-}$ species charge balanced by a mixture of Ca^{2+} and Mg^{2+} or Sr^{2+} and Mg^{2+}. However, fully magnesium substituted glass showed the presence of amorphous magnesium pyrophosphate, $Mg_2P_2O_7$.

- Magnesium substitution for calcium or for strontium in fluoro-phospho-aluminosilicate glasses led to increase in the amount of the five-coordinated aluminium species, Al(V), shown by ^{27}Al MAS-NMR.

- The fully magnesium substituted fluoro-phospho-aluminosilicate glass showed more polymerised silicate network with increased number of the bridging oxygen on SiO$_4$ tetrahedra compared to its calcium or strontium version.